# Enhancement of thermoelectric performance in strontium titanate by praseodymium substitution

A. V. Kovalevsky' , A. A. Yaremchenko, S. Populoh, A. Weidenkaff, and J. R. Frade

Citation: Journal of Applied Physics **113**, 053704 (2013); doi: 10.1063/1.4790307
View online: http://dx.doi.org/10.1063/1.4790307
View Table of Contents: http://aip.scitation.org/toc/jap/113/5
Published by the American Institute of Physics

# Enhancement of thermoelectric performance in strontium titanate by praseodymium substitution

A. V. Kovalevsky,[1,a)] A. A. Yaremchenko,[1] S. Populoh,[2] A. Weidenkaff,[2] and J. R. Frade[1]
[1]*Department of Materials and Ceramic Engineering, CICECO, University of Aveiro, 3810 193 Aveiro, Portugal*
[2]*EMPA, Solid State Chemistry and Catalysis, Ueberlandstr. 129, CH 8600 Duebendorf, Switzerland*

(Received 31 October 2012; accepted 17 January 2013; published online 1 February 2013)

In order to identify the effects of Pr additions on thermoelectric properties of strontium titanate, crystal structure, electrical and thermal conductivity, and Seebeck coefficient of $Sr_{1\ x}Pr_xTiO_3$ ($x = 0.02\ 0.30$) materials were studied at $400 < T < 1180$ K under highly reducing atmosphere. The mechanism of electronic transport was found to be similar up to 10% of praseodymium content, where generation of the charge carriers upon substitution resulted in significant increase of the electrical conductivity, moderate decrease in Seebeck coefficient, and general improvement of the power factor. Formation of point defects in the course of substitution led to suppression of the lattice thermal conductivity, whilst the contribution from electronic component was increasing with carrier concentration. Possible formation of layered structures and growing distortion of the perovskite lattice resulted in relatively low thermoelectric performance for $Sr_{0.80}Pr_{0.20}TiO_3$ and $Sr_{0.70}Pr_{0.30}TiO_3$. The maximum dimensionless figure of merit was observed for $Sr_{0.90}Pr_{0.10}TiO_3$ and amounted to ~0.23 at 670 K and ~0.34 at 1170 K, close to the values, obtained in similar conditions for the best bulk thermoelectrics, based on rare-earth substituted $SrTiO_3$. © *2013 American Institute of Physics*. [http://dx.doi.org/10.1063/1.4790307]

## I. INTRODUCTION

The development of environmentally friendly sources of the electrical power represents a challenging task for the energy sector worldwide. Since most of the energy (~60% 70%) used in the world is discharged as waste heat, "green" thermoelectric conversion received a considerable attention due to simplicity without employing moving parts, silent operation, and excellent scalability and reliability.[1–5] Although oxides have been considered ill suited for thermoelectric power generation,[2] the layered $Na_2CoO_4$ oxide was found to show high thermopower along with high electrical conductivity.[2,6] Since this discovery, many efforts were made on exploring new Co-containing oxides demonstrating high thermoelectric performance (Refs. 1 5 and references therein). At present time, particular interest is given to the transition metal-based mixed-conducting oxide materials, due to prospective thermoelectric properties (Refs. 3, 4, 7 9 and references therein), the absence of toxicity, and high natural abundance of the constituent compounds; the latter two issues represent their main advantages over the traditional thermoelectrics.

To develop feasible devices, thermoelectric modules should comprise both p-type and n-type semiconductor legs. For the time being, reasonably high performance was found mainly for p-type oxide thermoelectrics. The latter emphasizes a strong necessity in seeking highly performing n-type thermoelectric oxides. Among oxides, manganates[10,11] and strontium titanate $SrTiO_3$,[12,13] having perovskite-type lattice are considered promising thermoelectric materials. However, the bulk thermoelectric performance of pure $SrTiO_3$ is low, with wide band-gap and relatively high lattice thermal conductivity.[14] In recent years, many research efforts were focused on improving the n-type thermoelectric performance of $SrTiO_3$ by either A- or B-site donor substitution. In particular, addition of lanthanum or niobium proportionally increases the carrier concentration ($n$), resulting in higher electrical conductivity ($\sigma$) and lower Seebeck coefficient ($\alpha$).[14–20] Still, this leads to a general improvement of the power factor ($\sigma\alpha^2$). At low dopant content, the thermal conductivities of both $SrTi(Nb)O_3$ and $Sr(La)TiO_3$ were found to be almost independent on the carrier concentration.[15,16,18,19] Though further addition leads to unfavorable increase in the electronic contribution of thermal conductivity of $SrTi(Nb)O_3$,[16] improved phonon scattering provides overall decrease in thermal conductivity in the case of $Sr(La)TiO_3$.[17] The latter suggests donor substitution in A-sublattice as a promising strategy to suppress thermal conductivity, whilst increasing the electrical performance of strontium titanate. In fact, a comparison of several lanthanide ($Ln$) dopants (Y, La, Sm, Gd, Dy) has shown that the thermoelectric performance of $Sr_{0.9}Ln_{0.1}TiO_3$, described by dimensionless figure of merit $ZT$ ($\sigma\alpha^2 \times T/\kappa$), is mainly influenced by the changes in thermal conductivity, whilst electrical conductivity and Seebeck coefficient are almost independent on the type of $Ln$ cation.[20] Representative $ZT$ values for bulk polycrystalline thermoelectric oxides are 0.22 for $Sr_{0.9}Dy_{0.1}TiO_3$ at 573 K,[20] 0.28 for $Sr_{0.9}Nd_{0.1}TiO_3$ at 873 K,[21] 0.28 for $Sr_{0.88}La_{0.12}TiO_3$ at 773 K,[17] and even 0.36 for $La_{0.1}Sr_{0.83}Dy_{0.07}TiO_3$ at 1045 K,[22] or 0.4 at 1040 K for $EuTi_{0.98}Nb_{0.02}O_3$,[23] which are still fairly lower than required for feasible devices ($ZT > 1$).[24] Thus, further progress in

a)Author to whom correspondence should be addressed. Electronic mail: akavaleuski@ua.pt. Tel.: +351 234 370263. Fax: +351 234 370204.

 

improving *ZT* must rely on alternative ways such as micro- and nanostructural approaches.[4,5] At the same time, to our best knowledge, the impact of praseodymium substitution on thermoelectric properties of strontium titanate was not yet studied. Thus, the present work was focused on thermoelectric characterization of $Sr_{1-x}Pr_xTiO_3$ ($x = 0.02$, 0.05, 0.10, 0.20, 0.30) materials, sintered in highly reducing atmosphere.

## II. EXPERIMENTAL

The powders of $Sr_{1-x}Pr_xTiO_3$ ($x = 0.02$, 0.05, 0.10, 0.20, 0.30) were prepared by conventional solid state route using high-purity $SrCO_3$ (Sigma Aldrich, ≥99.9%), $Pr_6O_{11}$ (Sigma Aldrich, 99.9%), and $TiO_2$ (Sigma Aldrich, 99.8%). Prior to the weighing, titanium oxide was dried at 973 K for 2 h in air. The precursor mixtures were calcined consecutively at 1173 K, 1373 K, 1473, and 1576 K for 5 h at each temperature, with intermediate regrindings. After subsequent ball-milling with ethanol, disk-shaped ceramic samples were compacted uniaxially and sintered under different conditions. Samples with $x = 0.10$ 0.30 were sintered directly under reducing conditions, in flowing 10%$H_2$ 90%$N_2$ mixture, at 1773 K for 10 h. For the samples with lower praseodymium content, this upper temperature limit of the furnace was insufficient to prepare the ceramic samples with reasonable densities, under reducing conditions. Therefore, these samples were preliminarily sintered in air for 10 h at 2023 K and 1973 K for $x = 0.02$ and 0.05, respectively, and then reduced at 1773 K for 10 h in 10%$H_2$ 90%$N_2$ atmosphere. In the course of sintering/annealing, Pt foil or thick layer of the powder with same composition was used as substrates in air and hydrogen-based atmospheres, respectively, to avoid reaction with alumina supports.

The obtained disk samples were cut into rectangular bars for the measurements of total conductivity and Seebeck coefficient, or polished to provide uniform thickness (~1.00 mm) for thermal diffusivity measurements. Scanning electron microscopy (SEM) observations were performed on fracture surfaces; for X-ray diffraction (XRD) and specific heat capacity studies, the obtained ceramic samples were ground to powders in a mortar.

X-ray diffraction patterns were recorded using a Rigaku D/Max-B diffractometer ($CuK_\alpha$, $2\Theta = 10°$ 80°, step 0.02°, exposition 3 s). Unit-cell parameters were calculated from the diffraction data using profile matching method in FULLPROF software.[25] The experimental densities ($\rho$) of $Sr_{1-x}Pr_xTiO_3$ disk-shape ceramics were determined by geometrical measurements and weighing. Microstructural characterization was performed by SEM, using a Hitachi S-4100 instrument.

The total electrical conductivity and Seebeck coefficient were measured simultaneously using bar-shaped samples placed in specially developed alumina holder system. The measurement part of the setup is similar to that described in Ref. 26. The sample for thermopower measurement was fixed in vertical position by spring load force, in connection with two spiral Pt wires of S-type thermocouples, embedded in alumina capillaries and also acting as thermal voltage probes. In order to provide precise temperature control, the distance between sample ends and the thermocouple junctions did not exceed 1 mm. Temperature gradient along the length of the sample was set up by fine Pt wire heater, wound in the grooves of the holder at the top side. For the total conductivity measurements by four-probe DC technique, the second bar-shaped sample was placed in crosswise position in the vicinity of the middle part of the sample for thermopower measurement, in isothermal plane of the cell. The measurements were performed in 10%$H_2$ 90%$N_2$ mixture after equilibration at 473 1173 K, decreasing the temperature by steps 50 80 K. Whilst Seebeck coefficient measurements were performed at typical temperature gradients of 20 30 K, after each 2 3 steps the dependence of thermal voltage on the temperature gradient was verified in order to reveal and eliminate the effect of any voltage offset.[27] However, for all measured compositions, the contribution of the offset voltage into the measured thermal voltage was found to be less than 3%. As an example, Fig. 1 shows the voltage changes due to the applied temperature gradient, revealing a good linear response as well as negligible voltage at $\Delta T = 0$ K, if compared to that for $\Delta T = 20$ 30 K. The results of the Seebeck coefficient measurements were also corrected for the contribution of platinum wires. The criteria for equilibration of a sample after change in temperature included the relaxation rates of the conductivity and Seebeck coefficient less than 0.1%/min and 0.002 mV/(K min), respectively.

The thermal conductivity ($\kappa = D\rho c_p$) was determined indirectly by measurements of thermal diffusivity ($D$) (Netzsch LFA 457 Microflash), specific heat capacity ($c_p$) (Netzsch DSC 404 C), and density. The measurements were performed in flowing 5%$H_2$ 95%Ar mixture at 423 1173 K; the experimental procedure included stepwise (50 K) change in temperature, followed by dwell of 15 30 min for thermal equilibration of the sample. The estimated error in obtained values of thermal conductivity was less than 10% for all measured samples.

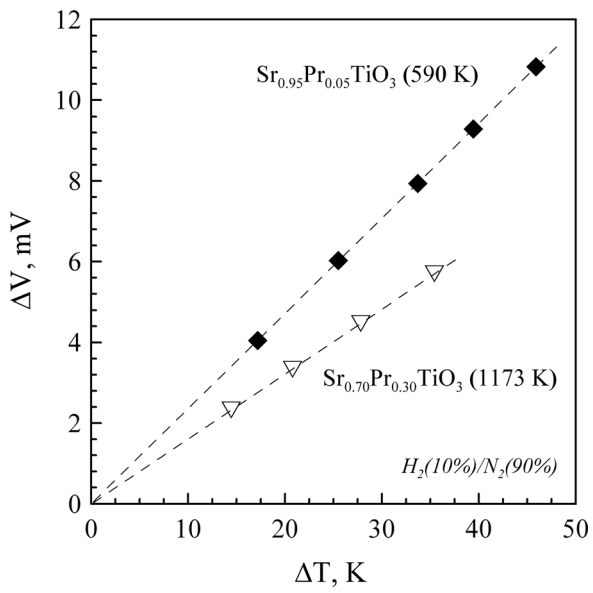


FIG. 1. Typical examples of thermal voltage changes in response to the applied temperature gradient in the setup, used for Seebeck coefficient studies.

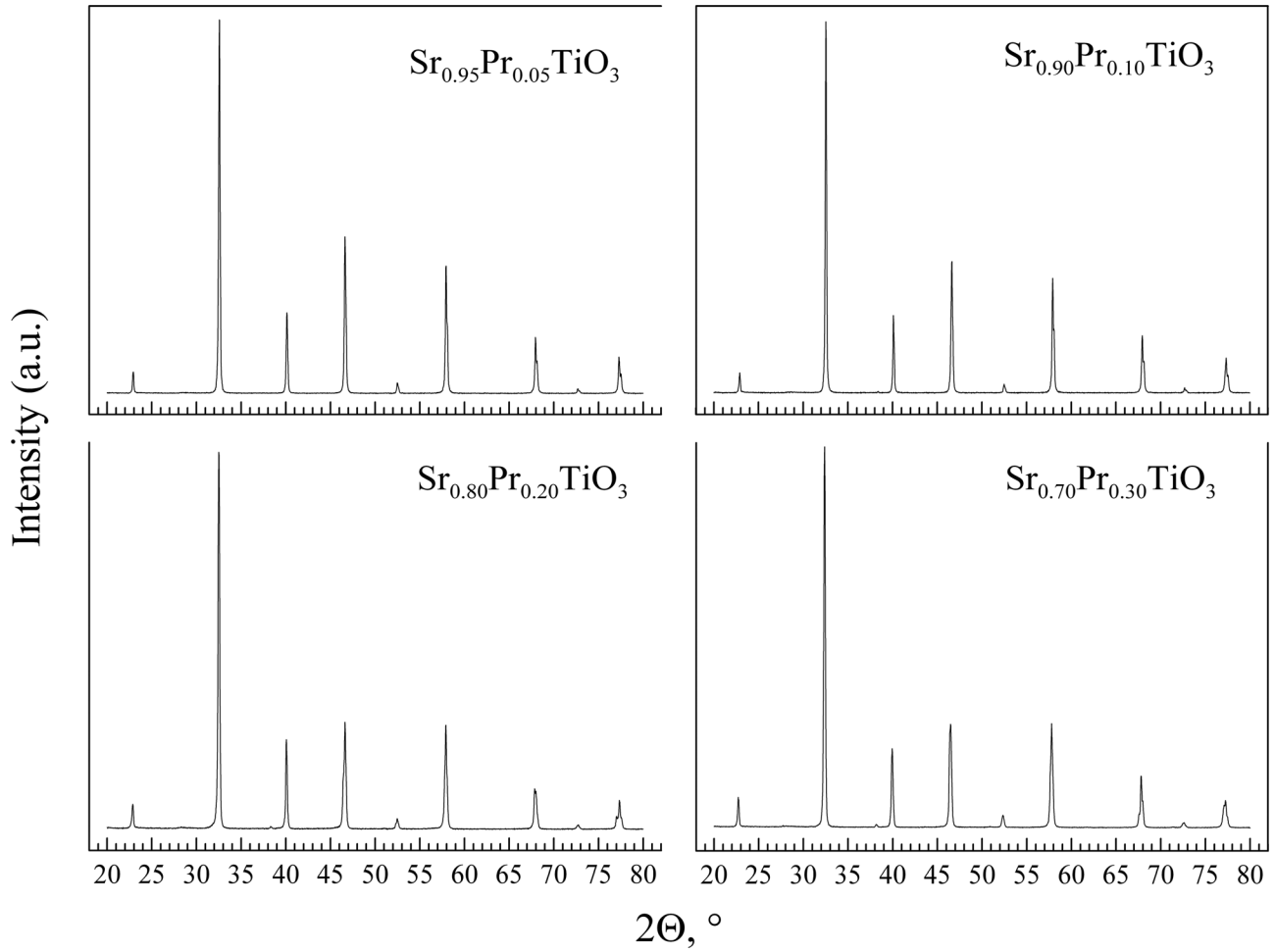


FIG. 2. XRD patterns of $Sr_{1-x}Pr_xTiO_3$ powdered samples at room temperature.

## III. RESULTS AND DISCUSSION

XRD analysis of the $Sr_{1-x}Pr_xTiO_3$ ($x = 0.02$, 0.05, 0.10, 0.20, 0.30) showed the formation of single-phase perovskite-type structure for all studied compositions (Fig. 2), corresponding lattice parameters are listed in Table I. The formation of cubic cell lattice with space group $Pm3m$ was observed for $x = 0.02$ and 0.05, in accordance with literature data.[28,29] Appearance of a weak reflection near $2\Theta \approx 38°$ for $0.10 \leq x \leq 0.20$, the intensity of which grows up with increasing praseodymium content, indicates change to tetragonal symmetry (space group $I4/mcm$), due to the significant difference in ionic radii between $Sr^{2+}$ and $Pr^{3+}/Pr^{4+}$ and corresponding distortion of $TiO_6$ octahedron.[29,30] The cubic unit cell volume slightly increases with Pr content from 59.66 to 59.71 Å$^3$ for $0.02 \leq x \leq 0.10$, in the case of $Sr_{0.90}Pr_{0.10}TiO_3$ pseudocubic lattice parameters were considered. Splitting of peaks at higher diffraction angles in XRD pattern of S70P30 composition suggests further decrease of lattice symmetry with Pr substitution. The pattern was, therefore, refined in orthorhombic symmetry using *Imma* space group, as was suggested for $Sr_{0.7}La_{0.3}TiO_{3+\delta}$.[31] Noteworthy that, even under reducing conditions, A-site substitution of $Sr^{2+}$ by $Pr^{3+}$ may result in oxygen excess in the samples, e.g., $Sr_{1-x}Pr_xTiO_{3+\delta}$. In this case, analogously to $(La,Sr)TiO_3$ system,[32,33] the prepared materials can be viewed as members of $A_nB_nO_{3n+2-\delta}$ series, mainly for the highest lanthanide contents ($x = 0.20$, 0.30). These structures can be described as perovskite slabs joined by crystallographic shears, where excess oxygen is accommodated. Also, for higher praseodymium concentrations, one should not exclude at least partial charge compensation via formation of Ruddlesden-Popper or SrO-rich secondary phases, though it typically takes place under oxidizing conditions (Ref. 34 and references therein). Although unambiguous detection of this phases by XRD analysis for the discussed Pr concentration range seems rather unlikely, their presence may noticeably contribute to the electrical and thermal properties, as discussed below.

According to the results of SEM analysis (Fig. 3) and density measurements (Table I), the sinterability of $Sr_{1-x}Pr_xTiO_3$ ceramics decreases for high praseodymium content $x = 0.20$, 0.30. At $0.02 \leq x \leq 0.10$, the formation of relatively dense ceramics was observed (Figs. 3(a) and 3(b)), whilst a representative micrograph for $Sr_{0.80}Pr_{0.20}TiO_3$ (Fig. 3(c)) indicates the formation of porous microstructure, with apparent porosity of ~23% (Table I). Since the porosity may have a significant effect on electrical and thermal conductivities, the experimental data for $\sigma$ and $\kappa$ were corrected, assuming that spherical pores are homogeneously distributed in the material, as described in Ref. 35.

TABLE I. Properties of $Sr_{1-x}Pr_xTiO_3$ ceramic samples.

| Chemical composition | Structure | Lattice parameters (Å) | Unit cell volume (Å$^3$) | Density (g/cm$^3$) | Relative density[a] (%) |
|---|---|---|---|---|---|
| $Sr_{0.98}Pr_{0.02}TiO_3$ | Cubic | a 3.9076(3) | 59.66(1) | 4.91 | 95.5 |
| $Sr_{0.95}Pr_{0.05}TiO_3$ | Cubic | a 3.9086(3) | 59.71(1) | 4.85 | 93.7 |
| $Sr_{0.90}Pr_{0.10}TiO_3$ | Tetragonal | a 5.5294(5)<br>c 7.8124(6) | 59.71(1)[b] | 5.15 | 98.0 |
| $Sr_{0.80}Pr_{0.20}TiO_3$ | Tetragonal | a 5.5190(3)<br>c 7.8363(4) | 238.69(2) | 4.14 | 76.6 |
| $Sr_{0.70}Pr_{0.30}TiO_3$ | Orthorhombic | a 5.5378(2)<br>b 7.7971(3)<br>c 5.5217(2) | 238.42(1) | 3.69 | 66.7 |

[a]Was calculated assuming that $\delta$ 0.
[b]Pseudocubic unit cell volume.

The temperature dependence of the total conductivity of $Sr_{1-x}Pr_xTiO_3$ ceramic samples is shown in Fig. 4. The conductivity increases with increasing praseodymium content up to $x = 0.10$, due to an increase in carrier concentration. In strongly reducing environments, the latter can be represented by the formation of defects according to the reaction

$$(x/2)Pr_2O_3 + (1-x)SrO + TiO_2 \xrightarrow{SrTiO_3} xPr^{\bullet}_{Sr} + (1-x)Sr^{x}_{Sr} + Ti^{x}_{Ti} + 3O^{x}_{O} + xe' + (x/4)O_2(g). \quad (1)$$

The electrical conductivity decreases with increasing temperature, indicating metallic conduction of the samples in the range of $0.02 \le x \le 0.10$. On the contrary, transition to semiconductor-type behaviour, followed by dramatic decrease in conductivity, was observed for $Sr_{0.80}Pr_{0.20}TiO_3$ and $Sr_{0.70}Pr_{0.30}TiO_3$. Most likely, for high praseodymium concentration, the formation of extended defects, where excess oxygen is accommodated (Eq. (2)), or charge compensation by simultaneous formation of strontium vacancies and rock-salt layers (Eq. (3)) may lead to appearance of localized electron states

$$(x/2)Pr_2O_3 + (1-x)SrO + TiO_2 \xrightarrow{SrTiO_3} xPr^{\bullet}_{Sr} + (1-x)Sr^{x}_{Sr} + Ti^{x}_{Ti} + 3O^{x}_{O} + (x/2)O''_{ex}, \quad (2)$$

$$(x/2)Pr_2O_3 + (1-x)SrO + TiO_2 \xrightarrow{SrTiO_3} xPr^{\bullet}_{Sr} + (1-1.5x)Sr^{x}_{Sr} + Ti^{x}_{Ti} + 3O^{x}_{O} + (x/2)V''_{Sr} + (x/2)SrO_{rs}. \quad (3)$$

At the same time, while smaller lattice volume provides higher overlapping of Ti-3 d orbitals, thus promoting delocalization of electrons and metallic-type conductivity variations with temperature,[36,37] observed for $0.02 \le x \le 0.10$, further increase in distortion of the perovskite lattice results in growing deviation of Ti-O-Ti bond angle from 180° and weakening of Ti-O bonds. The latter may also contribute to the dramatic change in conductivity mechanism. At higher temperatures, crystal lattice expansion may partially compensate the stresses, generated by Pr substitution, thus providing similar conductivity values for compositions with $x = 0.10$, 0.20, and 0.30, or even crossover of the results for $x = 0.1$ and $x \ge 0.2$.

Fig. 5 shows the temperature dependence of Seebeck coefficient for $Sr_{1-x}Pr_xTiO_3$ ceramics. The negative sign of $\alpha$ confirms n-type conductivity in all prepared samples. Over the whole measured temperature range, the Seebeck coefficient shows a trend to increase on heating. Similar type of $\alpha$ vs $T$ dependence was discussed for $Sr_{1-x}La_xTiO_3$ system on the basis of Boltzmann transport in a simplified parabolic band approach.[19] In general case, the relationship between the thermopower and carrier concentration can be given as $\alpha \approx \gamma - \ln(n)$,[17] where $\gamma$ is the scattering factor. Thus, the absolute values of Seebeck coefficient decrease with increasing Pr content due to the increase in carrier concentration. The results are consistent with those presented in literature for $Sr_{1-x}La_xTiO_3$ and $Sr_{1-x}Nd_xTiO_3$ systems,[17–21,38] also considering the magnitude of Seebeck coefficient. As an example, the $\alpha$ value of $-220\ \mu V/K$ at 1000 K, obtained in present work for $Sr_{0.90}Pr_{0.10}TiO_3$, in similar conditions is comparable to that of $Sr_{0.90}La_{0.10}TiO_3$ ($-220$ 245 $\mu V/K$)[20,38] and $Sr_{0.90}Nd_{0.10}TiO_3$ ($\sim -210\ \mu V/K$).[21] The latter, in particular, indicates that addition of Pr follows the similar trends with other rare-earth elements, regarding their effect on electrical properties of $SrTiO_3$. At the same time, an increase in electron localization upon Pr addition, having profound effect on the electrical conductivity changes with temperature (Fig. 4), may lead to a larger carrier effective mass. This influence, to a certain extent, may compensate the decrease in the Seebeck coefficient caused by the increase in carrier concentration, and thereby relatively large thermopower could be maintained even for high dopant content.[39] The latter may also be responsible for close values of $\alpha$, observed for $Sr_{0.80}Pr_{0.20}TiO_3$ and $Sr_{0.70}Pr_{0.30}TiO_3$ (Fig. 5).

The combined effect of electrical conductivity and Seebeck coefficient is illustrated by the temperature dependence of the power factor (Fig. 6). For $x \le 0.10$, the power factor exhibits similar behaviour with that observed for $Sr_{1-x}La_xTiO_3$ and $La_{0.1}Sr_{0.9-x}Dy_xTiO_3$ ceramics.[17,22,40] The maximum power factor of $\sim 1400\ \mu W\ m^{-1}\ K^{-1}$ at 670 K was observed for $Sr_{0.90}Pr_{0.10}TiO_3$, in accordance with the trends

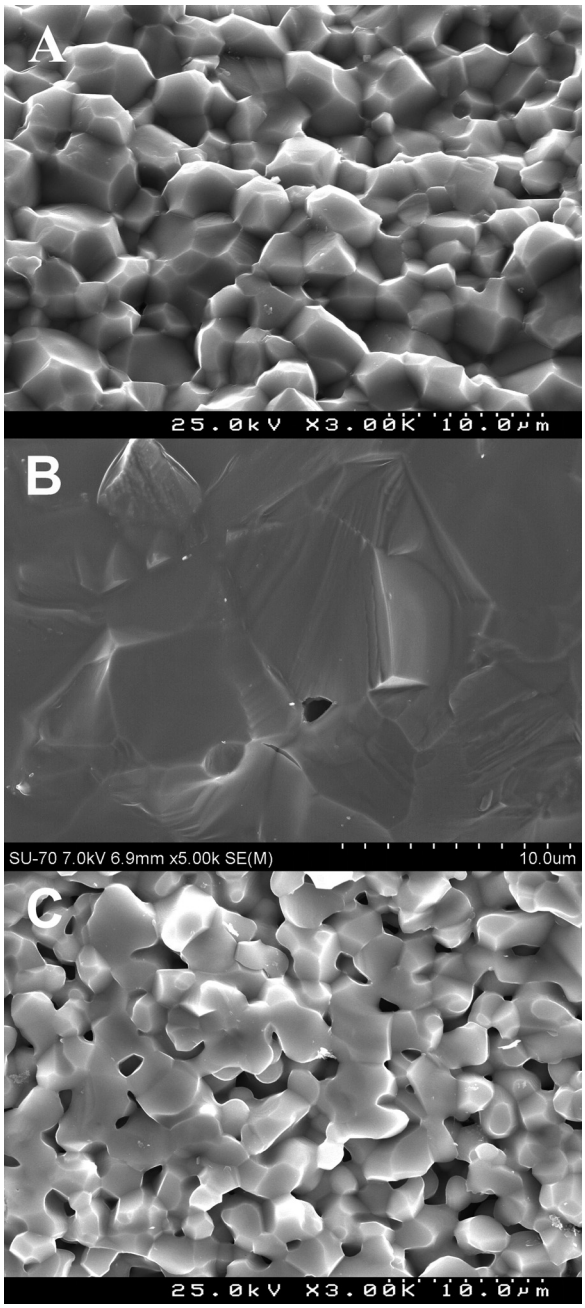


FIG. 3. SEM micrographs of the fractured ceramic $Sr_{1-x}Pr_xTiO_3$ samples with $x$ 0.02 (a), x 0.10 (b), and x 0.20 (c).

in total conductivity and Seebeck coefficient changes on adding praseodymium. This value is comparable with the maximum obtained for $Sr_{1-x}La_xTiO_3$[17] and noticeably higher than that for $La_{0.1}Sr_{0.9-x}Dy_xTiO_3$,[22] $Sr_{1-x}Ce_xTiO_3$,[41] and $Sr_{1-x}Y_xTiO_3$ materials.[42] The highest power factor of $Sr_{0.90}Pr_{0.10}TiO_3$ is provided by sharp increase in conductivity, whilst corresponding decrease in Seebeck coefficient is rather moderate. The results emphasize a high potential of substitution with praseodymium in approximate range of $x = 0.07$ 0.15 for improving the power factor of strontium titanate; for the latter, further optimization of praseodymium content is required. Despite relatively high Seebeck coefficient due to appearance of localized electron states, dramatic conductivity decrease at $x \geq 0.20$ is, in turn, responsible for

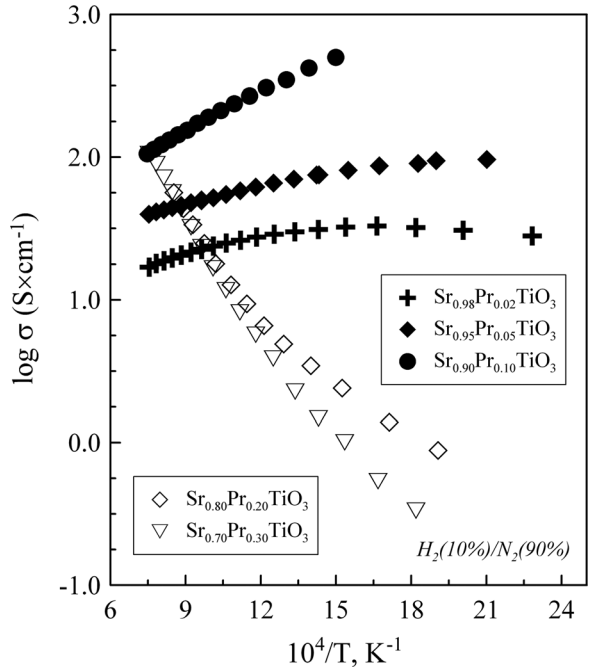


FIG. 4. Temperature dependence of the total conductivity of $Sr_{1-x}Pr_xTiO_3$ ceramics.

low $\sigma\alpha^2$ values, observed for the highest Pr contents in $Sr_{1-x}Pr_xTiO_3$ ceramic samples (Fig. 6).

The thermal conductivity of $Sr_{1-x}Pr_xTiO_3$ decreases with increasing temperature proportionally to $T^{-1}$, suggesting the prevailing role of lattice contribution (Fig. 7). For the $x \leq 0.10$, the thermal conductivity is weakly dependent on Pr content and slightly decreases with $x$. The impact of praseodymium additions can be analyzed considering two contributions to heat

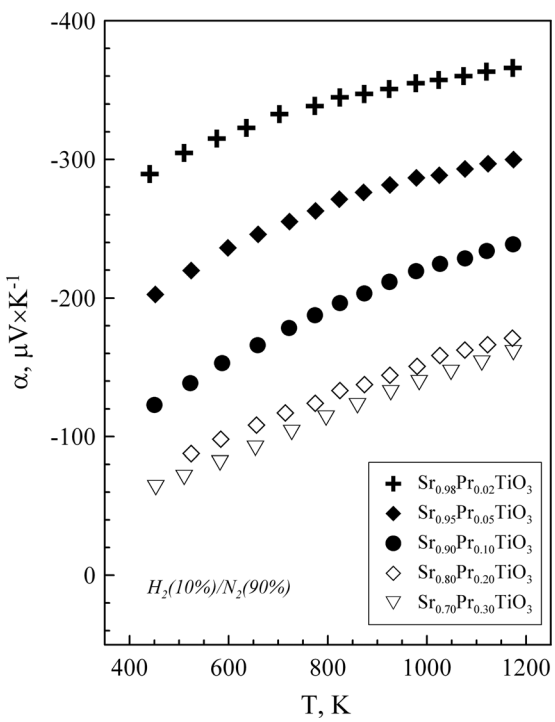


FIG. 5. Seebeck coefficient vs. temperature for $Sr_{1-x}Pr_xTiO_3$ ceramic samples.

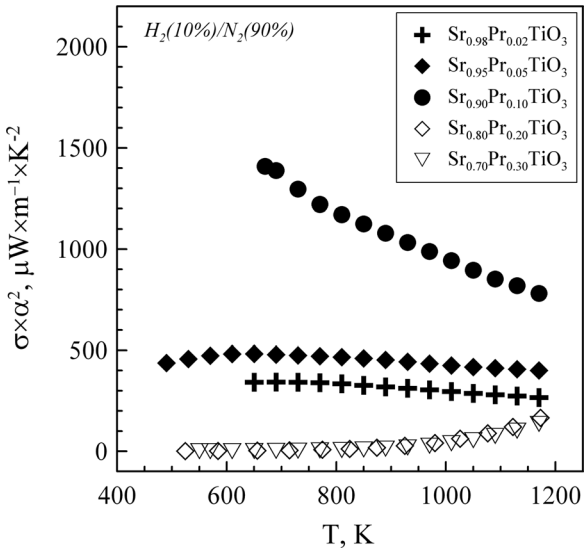


FIG. 6. Power factor of $Sr_{1-x}Pr_xTiO_3$ ceramics.

transfer in materials, namely, lattice contribution ($\kappa_{ph}$) and electronic component ($\kappa_{el}$)

$$\kappa = \kappa_{ph} + \kappa_{el}. \quad (4)$$

Electronic $\kappa_{el}$ can be estimated from Wiedemann-Franz's law as

$$\kappa_{el} = L\sigma T, \quad (5)$$

where L is the Lorenz number ($2.44 \times 10^{-8}\ V^2 \times K^{-2}$). The lattice thermal conductivity behaviour with temperature (Fig. 8(a)) is similar to that for $\kappa$ (Fig. 8(a)), again confirming the major contribution from $\kappa_{ph}$; for all studied materials, the electronic part was less than 20% (Fig. 8(b)). For $x \leq 0.10$, formation of point defects due to Pr addition is beneficial for improved phonon scattering and, thus, for lower lattice thermal conductivity, in agreement with the results obtained for various $(Sr,Ln)TiO_3$ materials.[17,21,42] In opposite to the negative effect on electronic conduction, distortion of perovskite

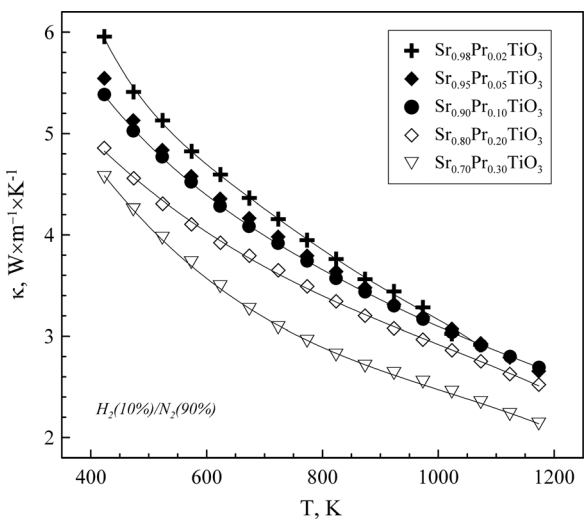


FIG. 7. Temperature dependence of the thermal conductivity of $Sr_{1-x}Pr_xTiO_3$ ceramic samples.

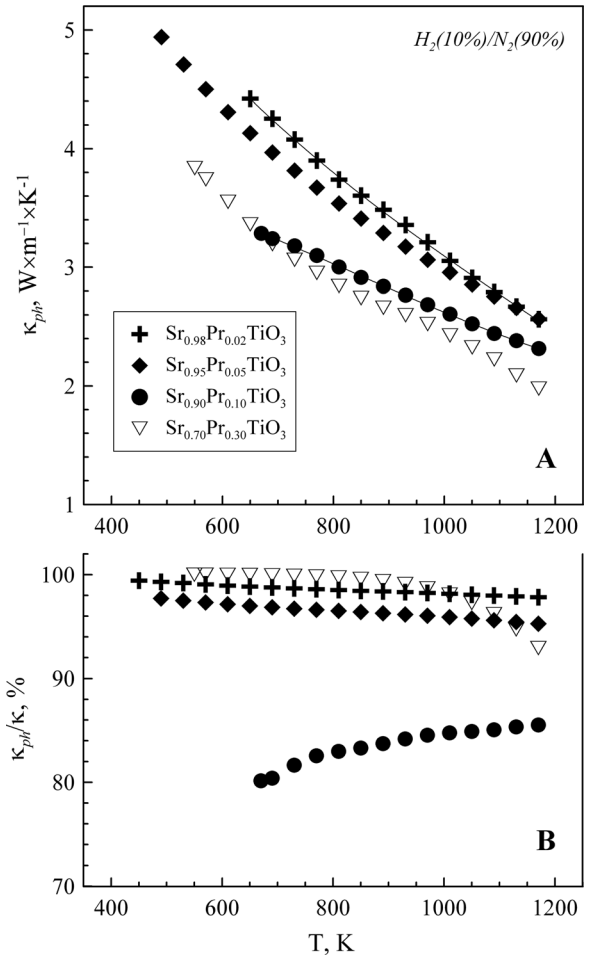


FIG. 8. Lattice thermal conductivity of $Sr_{1-x}Pr_xTiO_3$ (a) and its contribution to the total thermal conductivity (b).

lattice and weakening of Ti-O bonds may also provide stronger phonon-lattice interactions, resulting in lower $\kappa_{ph}$.[43] At the same time, the electronic thermal conductivity becomes significant at high carrier concentration: the $\kappa_{el}$ contribution to the thermal conductivity increases from 1% 5% for $x \leq 0.05$ up to 15% 20% in the case of $Sr_{0.90}Pr_{0.10}TiO_3$ (Fig. 8(b)). The latter, in particular, indicates that the positive effect of Pr on power factor and $\kappa_{ph}$ can be diminished by an increase in the electronic component of the thermal conductivity. Moreover, the lattice thermal conductivities of $Sr_{0.90}Pr_{0.10}TiO_3$ and $Sr_{0.70}Pr_{0.30}TiO_3$ are similar (Fig. 8(a)), suggesting that increasing praseodymium concentration above 10% does not yield further improvement in phonon scattering. However, one also should take into account relatively low densities, observed for $x \geq 0.20$ samples, which may lead to a certain overestimation of the thermal conductivity for $Sr_{0.80}Pr_{0.20}TiO_{3-\delta}$ and $Sr_{0.70}Pr_{0.30}TiO_{3-\delta}$.

Finally, Fig. 9 shows the temperature dependence of the dimensionless figure of merit *ZT* for $Sr_{1-x}Pr_xTiO_3$ ceramics. For $x \leq 0.10$, the *ZT* values increase with heating, following the same trend as observed in $Sr_{1-x}Nd_xTiO_3$ (Ref. 21) and $Sr_{0.9-x}Dy_xLa_{0.1}TiO_3$ (Ref. 22) systems. The maximum *ZT* corresponds to $Sr_{0.90}Pr_{0.10}TiO_3$ material and amounts to ~0.23 at 670 K and ~0.34 at 1170 K. These values are comparable to those obtained for the best bulk n-type thermoelectrics, based

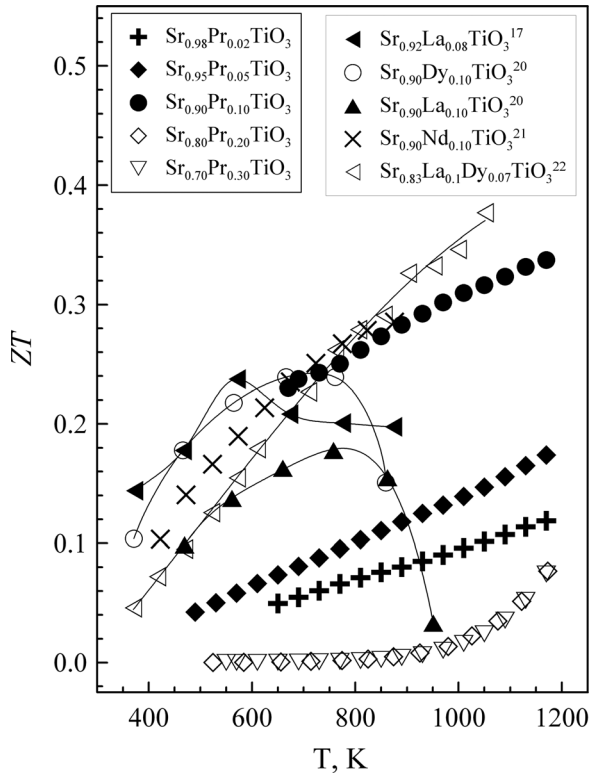


FIG. 9. Temperature dependence of the dimensionless figure of merit *ZT*.

on rare-earth substituted $SrTiO_3$ (Fig. 9). Although the figure of merit of $Sr_{0.90}Ln_{0.10}TiO_3$ was found to increase in the sequence La<Sm<Gd<Dy,[20] *ZT* values for $Sr_{0.90}Dy_{0.10}TiO_3$ (Ref. 20) and $Sr_{0.90}Pr_{0.10}TiO_3$ ceramics, obtained in present work, are similar up to 800 K, whilst at higher temperature the figure of merit of $Sr_{0.90}Pr_{0.10}TiO_3$ is significantly larger (Fig. 9). However, in this case, the comparison is, to a certain extent, ambiguous, since the discussed values for $Sr_{0.90}Dy_{0.10}TiO_3$ were obtained for material, sintered in Ar atmosphere, what may lead to underestimation of *ZT* in reducing conditions due to incomplete reduction. Apparently, the same reasons are responsible for noticeably lower *ZT* at $T > 700$ K, observed for $Sr_{0.92}La_{0.08}TiO_3$ (Ref. 17) and $Sr_{0.90}La_{0.10}TiO_3$.[20] On the contrary, the *ZT* of $Sr_{0.90}Pr_{0.10}TiO_3$ is close to that of $Sr_{0.90}Nd_{0.10}TiO_3$,[21] prepared in similar condition, although it should be lower, if assuming the relationship between nature of rare-earth cation and thermoelectric properties of $Sr_{0.90}Ln_{0.10}TiO_3$, found in Ref. 20. Thus, to understand deeper the effect of Pr additions, studied in present work, the influence of rare earth atomic mass and ionic radius on thermoelectric properties of $(Sr,Ln)TiO_3$ should be reassessed in strongly reducing conditions, where these materials show the highest performance. Simultaneous co-additions of La and Dy result in higher *ZT* at $T > 900$ K than that obtained for $Sr_{0.90}Pr_{0.10}TiO_3$. Therefore, one may foresee further improvement of the thermoelectric performance for Pr-substituted $SrTiO_3$ by the same strategy.

## IV. CONCLUSIONS

Ceramic $Sr_{1-x}Pr_xTiO_3$ ($x = 0.02$, 0.05, 0.10, 0.20, 0.30) materials were prepared by conventional solid state route, followed by sintering at 1773 K in highly reducing atmosphere. An increase in charge carrier concentration upon partial substitution of Sr by Pr was found to increase electrical conductivity and decrease Seebeck coefficient for $x \leq 0.10$, leading to general improvement of the power factor. Possible formation of layered structures and growing distortion of perovskite lattice resulted in low power factor for $Sr_{0.80}Pr_{0.20}TiO_3$ and $Sr_{0.70}Pr_{0.30}TiO_3$. Moderate addition of praseodymium was found promising for suppressing lattice thermal conductivity in strontium titanate. However, the positive effect of Pr substitution on power factor and lattice thermal conductivity can be diminished by an increase in the electronic component of the thermal conductivity. Maximum dimensionless figure of merit, comparable to those of the best bulk thermoelectrics, based on A-site donor substituted $SrTiO_3$, was observed for $Sr_{0.90}Pr_{0.10}TiO_3$ material. The results suggest Pr addition in $SrTiO_3$ as a promising strategy for seeking highly performing n-type thermoelectric oxides, where further improvement in performance may be achieved by co-additions of other rare-earth element and/or introduction of cation vacancies, aiming on enhancement of phonon scattering by lattice and suppressing the contribution of the electronic thermal conductivity.

## ACKNOWLEDGMENTS

This work was supported by the FCT, Portugal (Ciência-2008, Project No. PEst-C/CTM/LA0011/2011 and FCT Researcher 2012 program, Grant No. IF/00302/2012). Financial support from the SNF-NCCR Manep and the DfG-SPP thermoelectrics is greatly acknowledged. The authors are thankful to K. Galazka (EMPA) and S. Mikhalev, M. J. Pinho Bastos (UA) for their experimental assistance.

[1]D. M. Rowe, Int. J. Innov. Energy Syst. Power **1**, 13 (2006).
[2]T. Fujii and I. Terasaki, in *Chemistry, Physics, and Materials Science of Thermoelectric Materials: Beyond Bismuth Telluride*, edited by M. G. Kanatzidis, S. D. Mahanti, and T. P. Hogan (Kluwer Academic, New York, USA, 2003), pp. 71 87.
[3]I. Terasaki, M. Iwakawa, T. Nakano, A. Tsukuda, and W. Kobayashi, Dalton Trans. **39**, 1005 (2010).
[4]A. Weidenkaff, R. Robert, M. H. Aguirre, L. Bocher, and L. Schlapbach, Phys. Status Solidi (RRL) **1**, 247 (2007).
[5]M. S. Dresselhaus, G. Chen, M. Y. Tang, R. Yang, H. Lee, D. Wang, Z. Ren, J. P. Fleurial, and P. Gogna, Adv. Mater. **19**, 1043 (2007).
[6]I. Terasaki, Y. Sasago, and K. Uchinokura, Phys. Rev. B **56**, R12685 (1997).
[7]H. Hashimoto, T. Kusunose, and T. Sekino, J. Alloys Compd. **484**, 246 (2009).
[8]H. C. Wang, C. L. Wang, J. L. Zhang, W. B. Su, J. Liu, M. L. Zhao, N. Yin, Y. G. Lv, and L. M. Mei, Curr. Appl. Phys. **10**, 866 (2010).
[9]A. Weidenkaff, R. Robert, M. Aguirre, L. Bocher, T. Lippert, and S. Canulescu, Renewable Energy **33**, 342 (2008).
[10]L. Bocher, M. H. Aguirre, D. Logvinovich, A. Shkabko, R. R. Robert, M. Trottmann, and A. Weidenkaff, Inorg. Chem. **47**, 8077 (2008).
[11]A. Maignan, S. Hébert, L. Pi, D. Pelloquin, C. Martin, C. Michel, M. Hervieu, and B. Raveau, Cryst. Eng. **5**, 365 (2002).
[12]H. Ohta, Mater. Today **10**, 44 (2007).
[13]L. Bocher, M. H. Aguirre, R. Robert, M. Trottmann, D. Logvinovich, P. Hug, and A. Weidenkaff, Thermochim. Acta **457**, 11 (2007).
[14]A. Kinaci, C. Sevik, and T. Çağin, Phys. Rev. B **82**, 155114 (2010).
[15]S. Ohta, T. Nomura, H. Ohta, and K. Koumoto, J. Appl. Phys. **97**, 034106 (2005).
[16]S. Ohta, T. Nomura, H. Ohta, M. Hirano, H. Hosono, and K. Koumoto, Appl. Phys. Lett. **87**, 092108 (2005).

[17]P. P. Shang, B. P. Zhang, Y. Liu, J. F. Li, and H. M. Zhu, J. Electron. Mater. **40**, 926 (2011).
[18]L. Zhang, T. Tosho, N. Okinaka, and T. Akiyama, Mater. Trans. **48**, 1079 (2007).
[19]T. Okuda, K. Nakanishi, S. Miyasaka, and Y. Tokura, Phys. Rev. B **63**, 113104 (2001).
[20]H. Muta, K. Kurosaki, and S. Yamanaka, J. Alloys Compd. **350**, 292 (2003).
[21]J. Liu, C. L. Wang, W. B. Su, H. C. Wang, J. C. Li, J. L. Zhang, and L. M. Mei, J. Alloys Compd. **492**, L54 (2010).
[22]H. C. Wang, C. L. Wang, W. B. Su, J. Liu, Y. Zhao, H. Peng, J. L. Zhang, M. L. Shao, J. C. Liu, N. Yin, and L. M. Mei, Mater. Res. Bull. **45**, 809 (2010).
[23]L. Sagarna, A. Shkabko, S. Populoh, L. Karvonen, and A. Weidenkaff, Appl. Phys. Lett. **101**, 033908 (2012).
[24]T. M. Tritt, M. A. Subramanian, H. Bottner, T. Caillat, G. Chen, R. Funa hashi, X. Ji, M. Kanatzidis, K. Koumoto, G. S. Nolas, J. Poon, A. M. Rao, I. Terasaki, R. Venkatasubramanian, and J. Yang, MRS Bull. **31**, 188 (2006), and references cited therein.
[25]J. Rodríguez Carvajal, Physica B **192**, 55 (1993).
[26]M. V. Patrakeev, E. B. Mitberg, A. A. Lakhtin, I. A. Leonidov, V. L. Koz hevnikov, V. V. Kharton, M. Avdeev, and F. M. B. Marques, J. Solid State Chem. **167**, 203 (2002).
[27]S. Iwanaga, E. S. Toberer, A. LaLonde, and G. J. Snyder, Rev. Sci. Ins trum. **82**, 063905 (2011).
[28]A. Durán, E. Martínez, and J. M. Siqueiros, Integr. Ferroelectr. **71**, 115 (2005).
[29]R. Garg, A. Senyshyn, H. Boysen, and R. Ranjan, Phys. Rev. B **79**, 144122 (2009).
[30]A. Durán, F. Morales, L. Fuentes, and J. M. Siqueiros, J. Phys.: Condens. Matter **20**, 085219 (2008).
[31]M. Mori, K. Nakamura, and T. Itoh, J. Fuel Cell Sci. Technol. **9**, 021007 (2012).
[32]J. Canales Vázquez, M. J. Smith, J. T. S. Irvine, and W. Zhou, Adv. Funct. Mater. **15**, 1000 (2005).
[33]J. Canales Vázquez, S. W. Tao, and J. T. S. Irvine, Solid State Ionics **159**, 159 (2003).
[34]T. Kolodiazhnyi and A. Petric, J. Electroceram. **15**, 5 (2005).
[35]L. Zhang, T. Tosho, N. Okinaka, and T. Akiyama, Mater. Trans. **49**, 2868 (2008).
[36]H. Muta, A. Ieda, K. Kurosaki, and S. Yamanaka, Mater. Trans. **46**, 1466 (2005).
[37]J. B. Goodenough, J. Appl. Phys. **37**, 1415 (1966).
[38]R. Moos, A. Gnudi, and K. H. Hardtl, J. Appl. Phys. **78**, 5042 (1995).
[39]M. Ohtaki, J. Ceram. Soc. Jpn. **119**, 770 (2011).
[40]A. Kikuchi, L. Zhang, N. Okinaka, T. Tosho, and T. Akiyama, Mater. Trans. **50**, 2675 (2009).
[41]Y. F. Yamada, A. Ohtomo, and M. Kawasaki, Appl. Surf. Sci. **254**, 768 (2007).
[42]H. Obara, A. Yamamoto, C. H. Lee, K. Kobayashi, A. Matsumoto, and R. Funahashi, Jpn. J. Appl. Phys., Part 2 **43**, L540 (2004).
[43]Y. Wang, Y. Sui, P. Ren, L. Wang, X. Wang, W. Su, and H. J. Fan, Inorg. Chem. **49**, 3216 (2010).